Mitigation of friction-induced vibrations in braking systems: prediction of the mitigation limit

Baptiste Bergeot, Sergio Bellizzi, Sébastien Berger

Mitigation of friction-induced vibrations in braking systems: prediction of the mitigation limit

B. Bergeot [1], **S. Bellizzi** [2], **S. Berger** [1]
[1] INSA CVL, Univ. Orléans, Univ. Tours, LaMé EA 7494,
F-41034, 3 Rue de la Chocolaterie, CS 23410, 41034 Blois Cedex, France
e-mail: **baptiste.bergeot@insa-cvl.fr**

[2] Aix Marseille Univ, CNRS, Centrale Marseille, LMA UMR 7031, Marseille, France

Abstract
In this paper, we investigate a problem of passive mitigation of friction-induced vibrations due to mode coupling instability in breaking systems. For this purpose, the well-known Hultèn's model is coupled to one Nonlinear Energy Sinks (NES). In previous work by the authors [1], an asymptotic analysis has been performed on the system allowing to explain the steady-state response regimes observed in the numerical simulations and predict some of them. However, because of the appearance of a three-dimensional critical manifold, the prediction of the mitigation limit (i.e. the friction coefficient value which separates harmful situations from harmless situations) has been not performed. This present work completes this previous study using a general dynamics reduction method allowing to obtain one dimensional critical manifolds. The mitigation limit is therefore predicted and compared, for validation purposes, to numerical integration of the system.

1 Introduction

The squealing noise is due to dry friction in braking systems. It does not affect the quality of breaking but it is the source of significant noise nuisance. This phenomenon also called mode-coupling instability corresponds to a dynamic instability. It can be explained by the appearance of self-sustained oscillations - Limit Cycle Oscillation (LCO) - induced by dry friction and due to the coalescence of modes in self-excited systems.

Research is always active to understand the generation of a disc brake squeal and to predict and reduce it. Recent papers are for example based on non conventional analysis techniques such as probabilistic approach incorparing incertainty in the parameters of the model to predict instabilities [2, 3] or statistical approach from data obtained from different pad designs [4].

A more traditionally framework is considered here to investigate the problem of passive mitigation of friction-induced vibrations due to mode coupling instability in breaking systems. The well-known two degrees of freedom Hultèn's model is used as simplified analytic model to gain insight the mechanisms controlling brake squeal generation. This model is sufficient to investigate the mode-coupling instability ([5, 6, 7, 2]). This model is one of the models discussed in the review paper [8].

In the previous work by the authors [1], the mitigation squeaking noise was considered using the concept of Targeted Energy Transfer (TET)[9]. TET is a passive control method which consists in coupling an essentially nonlinear attachment also named Nonlinear Energy Sink (NES) to the primary system. The NES involves a mass, an essential cubic restoring force and a linear damping force. The addition of a NES drastically modifies the dynamic of the whole system giving access to complicate (nonlinear) dynamics

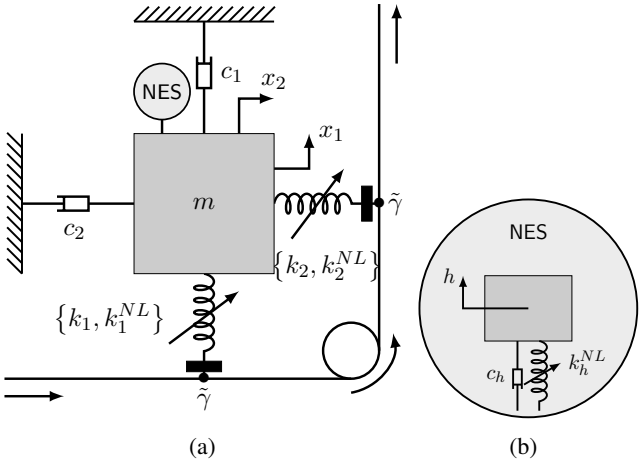

Figure 1: (a) Mechanical system with NES. (b) Zoom on the NES.

fostering the energy transfer from the primary system to the NES[10]. This phenomenon is called energy pumping.

Using the well-known Hultèn's model coupled to two ungrounded NESs, Bergeot et al. [1] showed that the use of NES appears to be an interesting way to control mode-coupling instability in braking systems. To analyze the steady-state response regimes, the system is partitioned in slow-fast dynamics using complexification-averaging approach due to the presence a small dimensionless parameter related to the mass of the NES. The slow-fast nature of the system allowed us to use multiple scale approach to analyze it. In particular, the shape of the Critical Manifold of the slow-flow and the associated stability properties provide an analytical tool to explain the existence of three regimes: periodic response regimes, strongly modulated responses regimes and no mitigation regimes that appear when the trivial solution is unstable. A complete suppression regimes is also observed.

The procedure gives access to the boundary values of the friction coefficient corresponding to the transition from complete suppression regime to periodic response regimes and from periodic response regimes to strongly modulated responses are predicted analytically. However the prediction of the boundary value between strongly modulated responses and no mitigation responses is not performed, this highlights that global structure of possible response regimes can not be deduced from local stability analysis of a slow flow subsystem with dimension larger than one. The prediction of this boundary value could be important in the context of engineering applications and this is the object of this present work.

The aim of the present work is i) to show that mode-coupling instability in braking systems can be mitigated with only one NES and ii) to provide an analytic prediction of the boundary value between strongly modulated responses and no mitigation responses.

The paper is organized as follows. In Sect. 2, the system under study including the Hultèn's model (the primary system) coupled to one ungrounded NES is presented and a reduction of the dynamics on the unstable mode of the primary system is performed. In Sect. 3 the reduced system is first analyzed following the Geometric Singular Perturbation Theory writting first the reduced system as a slow-flow system using a complexification-averaging method. Next the prediction of the mitigation limit is introduced and discussed when the friction parameter is used as a bifurcation parameter. Finally, analytical prediction proposed in Sect. 3 are compared to direct numerical simulations of the whole system.

2 System under study

2.1 Mechanical model

The system considered here is shown Fig. 1. It is composed by the simple 2 degrees-of-freedom (DOFs) self-excited system proposed by Hultèn [11] (the primary system) coupled to one NES with mass m_h, damping coefficient c_h and cubic stiffness coefficient k_h^{NL} (and without linear stiffness) attached on the system in an ungrounded configuration.

We focus on the analysis on the capacity of the NES attachments to suppress or mitigate vibrations when the primary system is unstable.

The system is decribed by the follwing equations:

$$\ddot{x}_1 + \epsilon\eta_1\dot{x}_1 + x_1 - \epsilon\gamma x_2 + \epsilon\varphi_1 x_1^3 + \epsilon\mu(\dot{x}_1 - \dot{h}_1) + \epsilon\alpha\left(x_1 - h_1\right)^3 = 0 \tag{1a}$$

$$\ddot{x}_2 + \epsilon\eta_2\dot{x}_2 + (1 - 2\epsilon a)x_2 + \epsilon\gamma x_1 + \epsilon\varphi_2 x_2^3 = 0 \tag{1b}$$

$$\epsilon\ddot{h} + \epsilon\mu(\dot{h} - \dot{x}) + \epsilon\alpha\left(h - x_1\right)^3 = 0 \tag{1c}$$

where x_1 and x_2 (respectively h) are the displacements of the primary mass (respectively of the NES mass).

As shwon in [1], Eq. (1) results from a scaling of time ($t = \omega_1\tilde{t}$ with $\omega_1^2 = k_1/m$) and a scaling of the parameters with respect to the mass ratio $\epsilon = m_h/m$ assuming $0 < \epsilon << 1$ where coefficients η_1, η_2, φ_1, φ_2, γ, μ, α, a are adopted to be of order unity. The coefficients η_1 and η_2 characterize the damping terms (c_1, c_2) of the Hulten model, φ_1 and φ_2 are the associated cubic stiffness coefficients (k_1^{NL}, k_2^{NL}) whereas γ is the friction coefficient. The parameters μ and α characterize the damping coefficient (c_h)and the cubic stiffness coefficient (k_h^{NL}) of the NES. Finally, the coefficient a is defined as $\sqrt{k_2/k_1} = 1 - \epsilon a$.

2.2 Reduction of the dynamics

To simplify asymptotic analysis in next section, it is convenient to introduce new coordinates as

$$u_1 = x_1 + \epsilon\, h \qquad u_2 = x_2 \qquad v = x_1 - h, \tag{2a}$$

giving reciprocally,

$$x_1 = \frac{u_1 + \epsilon\, v}{1 + \epsilon} \qquad x_2 = u_2 \qquad h = \frac{u_1 - v}{1 + \epsilon}. \tag{3a}$$

Using Eqs. (3), Eq. (1) is transformed into the following form

$$\ddot{u}_1 + \epsilon\eta_1\dot{u}_1 + u_1 - \epsilon\gamma u_2 + \epsilon(\varphi_1 u_1^3 - u_1 + v) = 0 \tag{4a}$$

$$\ddot{u}_2 + \epsilon\eta_2\dot{u}_2 + (1 - 2\epsilon a)u_2 + \epsilon\gamma u_1 + \epsilon\varphi_2 u_2^3 = 0 \tag{4b}$$

$$\ddot{v} + (1 + \epsilon)\mu\dot{v} + \epsilon v + (1 + \epsilon)\alpha v^3 + \epsilon\eta_1\dot{u}_1 + (1 - \epsilon)u_1 - \epsilon\gamma u_2 + \epsilon\varphi_1 u_1^3 = 0, \tag{4c}$$

where a first-order Taylor series around $\epsilon = 0$ has been performed.

The reduction of the dynamics is performed on the first two equations of Eqs. (4) (the primary system) using the biorthogonal transformation (see for example [12]).

Let $\mathbf{u} = (u_1, u_2, \dot{u}_1, \dot{u}_2)^t$ (the " ^{t} " is the usual notation for transpose operator), Eqs. (4a) and (4b) can be written as a system of first order differential equations (state-space form)

$$\dot{\mathbf{u}} = \mathbf{A}\mathbf{u} + \epsilon\mathbf{f}\left(\mathbf{u}, v\right), \tag{5}$$

where the matrix $\mathbf{A}$ is defined by

$$\mathbf{A} = \begin{bmatrix} 0 & 0 & 1 & 0 \\ 0 & 0 & 0 & 1 \\ -1 & \gamma\epsilon & -\epsilon\eta_1 & 0 \\ -\gamma\epsilon & -1+2a\epsilon & 0 & -\epsilon\eta_2 \end{bmatrix} \tag{6}$$

and the vector function $\mathbf{f}$ is easily deduced from Eqs. (4a) and (4b). It is important to note that the matrix $\mathbf{A}$ also characterizes the linear part of the primary system written on its state-space form.

The following eigenvalue problems:

$$\mathbf{A}\mathbf{r} = \lambda\mathbf{r} \quad \text{and} \quad \mathbf{A}^t\mathbf{l} = \lambda\mathbf{l}, \tag{7}$$

where $\mathbf{A}^t$ denotes the transpose of $\mathbf{A}$, are solved giving:

- two pairs of complex conjugates eigenvalues: λ_1 and λ_1^*, and λ_2 and λ_2^* (the " * " is the usual notation for the complex conjugate),
- two pairs of complex conjugates eigenvectors of $\mathbf{A}$: $\mathbf{r}_1$ and $\mathbf{r}_1^*$, and $\mathbf{r}_2$ and $\mathbf{r}_2^*$, called *right eigenvectors* of $\mathbf{A}$,
- two pairs of complex conjugates eigenvectors of $\mathbf{A}^t$: $\mathbf{l}_1$ and $\mathbf{l}_1^*$, and $\mathbf{l}_2$ and $\mathbf{l}_2^*$, called *left eigenvectors* of $\mathbf{A}$.

The right and left eigenvectors satisfy the biorthogonality properties i.e $\mathbf{L}^t\mathbf{R}$ and $\mathbf{L}^t\mathbf{A}\mathbf{R}$ are diagonal matrices where $\mathbf{R} = [\mathbf{r}_1\ \mathbf{r}_1^*\ \mathbf{r}_2\ \mathbf{r}_2^*]$ and $\mathbf{L} = [\mathbf{l}_1\ \mathbf{l}_1^*\ \mathbf{l}_2\ \mathbf{l}_2^*]$. It is convenient to normalize the two sets of eigenvectors $\mathbf{r}_i$ and $\mathbf{l}_i$ in order to obtain

$$\mathbf{L}^t\mathbf{R} = \mathbf{I} \quad \text{giving} \quad \mathbf{L}^t\mathbf{A}\mathbf{R} = \mathbf{D} \tag{8}$$

where $\mathbf{I}$ is the identity matrix and $\mathbf{D} = \mathrm{diag}(\lambda_1, \lambda_1^*, \lambda_2, \lambda_2^*)$.

Performing now the change of variables

$$\mathbf{u} = \mathbf{R}\mathbf{q} \ \text{ or equivalently } \ \mathbf{q} = \mathbf{L}^t\mathbf{u}, \tag{9}$$

Eq. (5) becomes

$$\dot{\mathbf{q}} = \mathbf{D}\mathbf{q} + \epsilon\mathbf{L}^t\mathbf{f}\left(\mathbf{R}\mathbf{u}, v\right). \tag{10}$$

Eqs. (10) and (4c), which are equivalent to Eqs. (4), define the Full Non-Averaged System (FNAS).

From now we assume that only one pair of eigenvalues of the perturbed system, here denoted without lost of generality (λ_1, λ_1^*), may have positive real part whereas the second pair (λ_2, λ_2^*) always has negative real part. Hence, and because the coupling terms are of the order of magnitude of ϵ, after some exponentially decaying transients the components q_2, q_2^* become small, i.e. $q_2 \sim q_2^* \sim O(\epsilon)$. Therefore, all terms related to q_2, q_2^* can be omitted from further consideration and Eq. (10) becomes

$$\dot{q}_1 = \lambda_1 q_1 + \epsilon\mathbf{l_1}\mathbf{f}\left(\mathbf{r}_{11}q_1 + \mathbf{r}_{11}^*q_1^*, v\right) \tag{11}$$

where $\mathbf{r}_{11}$ denotes the first component of the vector $\mathbf{r}_1$.

Eqs. (11) and (4c) define the reduced equations of motion. Note that the previous reduction is valid during transient when the amplitudes are relatively small and therefore must be questioned when large amplitudes of oscillation are reached.

2.3 About the order of magnitude of the eigenvalues and eigenvectors

Looking at Eq. (6), the matrix $\mathbf{A}$ appears as a perturbed matrix $\mathbf{A} = \mathbf{A}_0 + \epsilon\mathbf{A}_1$ where the matrix $\mathbf{A}_1$ results from the damping and friction forces. The perturbed system (5) is a circulatory system [1] while the unperturbed system, defined by $\mathbf{A}_0$ is not. It can be shown that $\mathbf{A}$ is regularly perturbed with respect to its eigenvalues. Indeed, the determinant $\det(\mathbf{A})$ do not contain singular terms. Therefore, the matrix $\mathbf{D}$ can be written as follow $\mathbf{D} = \mathbf{D}_0 + \epsilon\mathbf{D}_1$, where $\mathbf{D}_0 = \mathrm{diag}(j, -j, j, -j)$ (from now, $j^2 = -1$) is a diagonal matrix with the eigenvalues of $\mathbf{A}_0$ on its diagonal and $\mathbf{D}_1 \sim O(1)$. On the contrary, the perturbed system is no regularly perturbed with respect to its eigenvectors, i.e. the eigenvectors of $\mathbf{A}$ do not tend toward the eigenvectors of $\mathbf{A_0}$ when $\epsilon \to 0$. Consequently, as the most restrictive assumption for further analysis, we assume that left and right eigenvectors are of order 1 (i.e. $\mathbf{R}, \mathbf{L} \sim O(1)$), even if they can contain terms of order ϵ.

Taking into account previous remarks, the eigenvalue λ_1 is written as follows

$$\lambda_1 = j + \epsilon\left(\rho_u + j\nu_u\right) = \epsilon\rho_u + j\left(1 + \epsilon\nu_u\right), \tag{12}$$

where $1 + \epsilon\nu_u$ is the frequency for which the observed steady-state responses are assumed to oscillate and the real part is of order ϵ (i.e. $\rho_u \sim O(1)$). Therefore, Eq. (11) becomes

$$\dot{q}_1 = jq_1 + \epsilon\left(\rho_u + j\nu_u\right)q_1 + \epsilon\mathbf{l_1}\mathbf{f}\left(\mathbf{r}_{11}q_1 + \mathbf{r}_{11}^*q_1^*, v\right). \tag{13}$$

Finally grouping Eqs. (13) and (4c), the reduced equations of motion take the following form

$$\begin{aligned}\dot{q}_1 - jq_1 - \epsilon\left(\rho_u + j\nu_u\right)q_1 - \epsilon\mathbf{l}_{31}\left(\varphi_1(\mathbf{r}_{11}q_1 + \mathbf{r}_{11}^*q_1^*)^3 - \left(\mathbf{r}_{11}q_1 + \mathbf{r}_{11}^*q_1^*\right)\right) + \\ \epsilon\mathbf{l}_{41}\varphi_2(\mathbf{r}_{21}q_1 + \mathbf{r}_{21}^*q_1^*)^3 + \epsilon\mathbf{l}_{31}v = 0 \qquad (14a)\\ \ddot{v} + (1+\epsilon)\mu\dot{v} + \epsilon v + (1+\epsilon)\alpha v^3 + \epsilon\eta_1(\mathbf{r}_{31}q_1 + \mathbf{r}_{31}^*q_1^*) + (1-\epsilon)(\mathbf{r}_{11}q_1 + \mathbf{r}_{11}^*q_1^*) - \\ \epsilon\gamma(\mathbf{r}_{21}q_1 + \mathbf{r}_{21}^*q_1^*) + \epsilon\varphi_1(\mathbf{r}_{11}q_1 + \mathbf{r}_{11}^*q_1^*)^3 = 0, \qquad (14b)\end{aligned}$$

where $\mathbf{r}_{ij}$ (respectively $\mathbf{l}_{ij}$) denotes the i-th component of the vector $\mathbf{r}_j$ (respectively $\mathbf{l}_j$). Note that Eqs. (14) characterize one unknown complex variable q_1 and one unknown real variable v. Eqs. (14) define the Reduced Non-Averaged System (RNAS).

3 Asymptotic analysis of the reduced system

3.1 The slow-flow

In this section, RNAS (14) is analyzed following the *Geometric Singular Perturbation Theory* (GSPT) ([13, 14]) writing first the system as a slow-flow system.

The following change of variables is first applied to complexify the variable v as

$$\psi = \dot{v} + jv \tag{15a}$$

and the complex variables q_1, and ψ are next replaced by

$$q_1 = \phi e^{jt} \tag{16a}$$

$$\psi = \xi e^{jt}, \tag{16b}$$

where ϕ and ξ are the complex slow modulated amplitude of the fast component e^{jt}.

[1] A circulatory mechanical system has a non-symmetric stiffness matrix due for example to friction or follower forces.

After some algebraic manipulations followed by an averaging over one period $T = 2\pi$ of the resulting equations, Eqs. (14) reduce to

$$\dot{\phi} = \epsilon \left(\left(\rho_u - j\nu_u + \mathbf{l}_{31}\mathbf{r}_{11}\right)\phi - 3\left(\mathbf{l}_{31}|\mathbf{r}_{11}|^2\mathbf{r}_{11}\varphi_1 + \mathbf{l}_{41}|\mathbf{r}_{21}|^2\mathbf{r}_{21}\varphi_2\right)|\phi|^2\phi + \frac{j\mathbf{l}_{31}}{2}\xi \right) \tag{17a}$$

$$\begin{aligned}\dot{\xi} = &-\mathbf{r}_{11}\phi - \frac{1}{2}(\mu + j\omega_u)\xi + \frac{3j\alpha}{8}|\xi|^2\xi \\ &+ \epsilon\left(\left(\mathbf{r}_{11} + \gamma\mathbf{r}_{21} - \eta_1\mathbf{r}_{31}\right)\phi - \frac{1}{2}(\mu - j)\xi - 3|\mathbf{r}_{11}|^2\mathbf{r}_{11}\varphi_1|\phi|^2\phi + \frac{3j\alpha}{8}|\xi|^2\xi \right).\end{aligned} \tag{17b}$$

where $|.|$ denotes the modulus of a complex number.

For the future analysis, it is convenient to rewrite Eqs. (17) considering real variables. To achieve this, polar coordinates are introduced as

$$\phi = se^{j\theta_\phi} \tag{18a}$$

$$\xi = re^{j\theta_\xi}, \tag{18b}$$

where s and θ_ϕ (respectivily r and θ_ξ) characterized the modulus and the argument of ϕ (respectivaly ξ). Substituting Eq. (18b) into Eq. (17) and separting in real and imaginary part, Eq. (17) reduce to

$$\dot{s} = \epsilon f(s, r, \delta) \tag{19a}$$

$$\dot{r} = g_1(s, r, \delta, \epsilon) \tag{19b}$$

$$\dot{\delta} = g_2(s, r, \delta, \epsilon), \tag{19c}$$

where $\delta = \theta_\phi - \theta_\xi$. The expressions of the functions f, g_1 and g_2 are given Appendix A.

Eqs. (19) appear to have the slow-fast form where s is the slow variable whereas r and δ are the fast variables. Eqs. (19) can be reformulated by switching from the *fast* time scale t to the *slow* time scale $\tau = \epsilon t$ giving

$$s' = f\left(s, r, \delta\right) \tag{20a}$$

$$\epsilon\, r' = g_1\left(s, r, \delta, \epsilon\right) \tag{20b}$$

$$\epsilon\, \delta' = g_2\left(s, r, \delta, \epsilon\right), \tag{20c}$$

where $' = \frac{d}{d\tau}$. Solutions of slow-fast system (19) or (20) can exhibit slow and fast epochs characterized by slow and fast motions. This will be considered in the following Section in the framework of the GSPT.

3.2 The Critical Manifold and its stability

Stating $\epsilon = 0$, Eqs. (19) and (20) reduce, respectively, to:

$$\dot{s} = 0 \tag{21a}$$

$$\dot{r} = g_1(s, r, \delta, 0) \tag{21b}$$

$$\dot{\delta} = g_2(s, r, \delta, 0), \tag{21c}$$

the *fast subsystem* which is a family of dynamical systems for the fast variables ξ and

$$s' = f\left(s, r, \delta\right) \tag{22a}$$

$$0 = g_1\left(s, r, \delta, 0\right) \tag{22b}$$

$$0 = g_2\left(s, r, \delta, 0\right), \tag{22c}$$

the *slow subsystem* which is a system of Differential Algebraic Equations (DAE). The goal of the GSPT is to characterize the dynamic of the initial system (19) or (20) using the fast and slow subsystems (21) or (22).

Considering the slow subsystem, the nonlinear equations (22b) and (22c) define the so-called *Critical Manifold* S as [14]

$$S := \left\{ (s, r, \delta) \in R^3 \mid g_1(s, r, \delta, 0) = 0 \text{ and } g_2(s, r, \delta, 0) = 0 \right\}. \tag{23}$$

Looking at Eqs. (42) and (43), the nonlinear equations takes the form

$$g_1(s, r, \delta, 0) = -\frac{\mu}{2} r - (\mathbf{r}_{11}^R \cos(\delta) - \mathbf{r}_{11}^I \sin(\delta)) s = 0 \tag{24a}$$

$$g_2(s, r, \delta, 0) = \frac{3\alpha}{8} r^2 - \frac{\omega_u}{2} - (\mathbf{r}_{11}^R \sin(\delta) + \mathbf{r}_{11}^I \cos(\delta)) \frac{s}{r} = 0. \tag{24b}$$

Combining Eqs. (24a) and (24b) leads to the modulus equation

$$s^2 \left(\mathbf{r}_{11}^{R^2} + \mathbf{r}_{11}^{I^2} \right) = H(r), \tag{25}$$

where

$$H(r) = H_1^2(r) + H_2(r)^2 \qquad \text{with} \qquad H_1(r) = -\frac{\mu}{2} r \qquad \text{and} \qquad H_2(r) = \left(\frac{3\alpha}{8} r^2 - \frac{1}{2} \right) r, \tag{26}$$

and to the characterization of the argument δ as

$$\cos(\delta) = \frac{r \left(3r^2 \alpha \mathbf{r}_{11}^R + 4\mu \mathbf{r}_{11}^I - 4\mathbf{r}_{11}^R \right)}{8s \left(\mathbf{r}_{11}^{R^2} + \mathbf{r}_{11}^{I^2} \right)} \qquad \text{and} \qquad \sin(\delta) = \frac{r \left(3r^2 \alpha \mathbf{r}_{11}^R - 4\mu \mathbf{r}_{11}^R - 4\mathbf{r}_{11}^I \right)}{8s \left(\mathbf{r}_{11}^{R^2} + \mathbf{r}_{11}^{I^2} \right)}. \tag{27}$$

Hence the Critical Manifold S appears to be a curve in the (s, r)-plane.

Stability analysis of the SIM is now carry out considering the fast subsystem (21). It can be shown that the Jacobian matrix reads as

$$\begin{bmatrix} \dfrac{dH_1(r)}{dr} & -H_2(r) \\ \dfrac{1}{r} \dfrac{dH_2(r)}{dr} & \dfrac{H_1(r)}{r} \end{bmatrix}, \tag{28}$$

and using the Routh-Hurwitz criterium we can deduce that a fixed point of Eq. (21) is stable if $H'(r) > 0$ and unstable if $H'(r) < 0$. Hence the subset of S satisfying $H'(r) > 0$ defines the attractive zone for the fast dynamics whereas the subset of S satisfying $H'(r) > 0$ define the repulsive zone.

Exploiting the polynomial properties of H, it can be shown that the local extrema of H (i.e $H'(r) = 0$) occur at

$$r^M = \frac{2}{3\sqrt{\alpha}} \sqrt{2 - \sqrt{1 - 3\mu^2}} \qquad \text{and} \qquad r^m = \frac{2}{3\sqrt{\alpha}} \sqrt{2 + \sqrt{1 - 3\mu^2}}, \tag{29}$$

if the following relation holds

$$\mu < \frac{1}{\sqrt{3}}, \tag{30}$$

and in this case $r^M < r^m$.

When condition (30) is satisfied, the two points (s^m, r^m) and (s^M, r^M) where the two scalars s^M and s^m are defined by $s^m = \sqrt{\frac{H(r^m)}{\mathbf{r}_{11}^{R^2} + \mathbf{r}_{11}^{I^2}}}$ and $s^M = \sqrt{\frac{H(r^M)}{\mathbf{r}_{11}^{R^2} + \mathbf{r}_{11}^{I^2}}}$ characterize the bounds where S ceases to be attractive connecting stable and unstable (repulsive) parts of S. These two points are called *fold points*. A typical CM is depicted Fig. 2 where the green points correspond to the fold points. The two scalars r^d and r^u (see the red points on Fig. 2), which will be used later, are defined by $H_n(r_n^m) = H_n(r_n^d)$ and $H_n(r_n^M) = H_n(r_n^u)$ giving

$$r_n^d = \frac{2\sqrt{2}}{3\sqrt{\alpha}} \sqrt{1 - \sqrt{1 - 3\mu^2}} \qquad \text{and} \qquad r_n^u = \frac{2\sqrt{2}}{3\sqrt{\alpha}} \sqrt{1 + \sqrt{1 - 3\mu^2}}. \tag{31a}$$

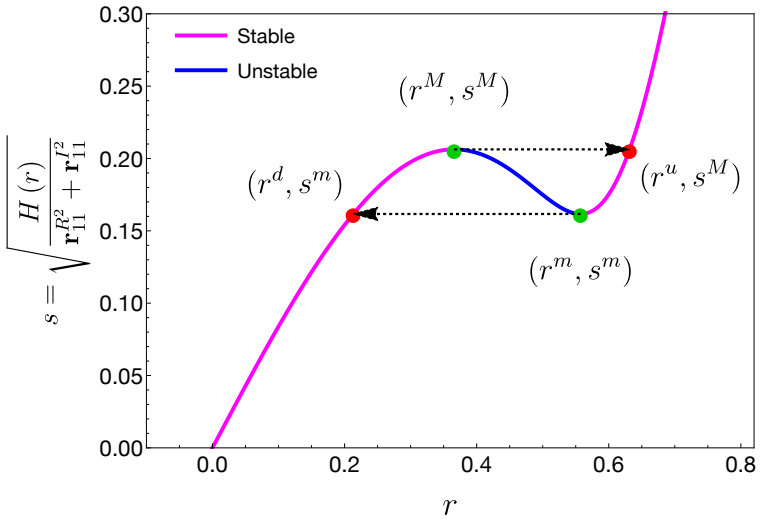

Figure 2: Typical *Critical Manifold* (CM). Set of parameters (40) is used with $\mu = 0.35$.

3.3 Fixed points and folded singularities of the slow flow

The dynamic of the slow subsystem (22) is now characterized in S.

Substituting Eq. (25) into Eq. (22a) results in

$$\left(\sqrt{\frac{H(r)}{\mathbf{r}_{11}^{R2} + \mathbf{r}_{11}^{I2}}}\right)' = f\left(\sqrt{\frac{H(r)}{\mathbf{r}_{11}^{R2} + \mathbf{r}_{11}^{I2}}}, r, \delta\right) \tag{32}$$

Next using Eq. (22b), Eq. (32) reduces to

$$\frac{dH(r)}{dr} r' = f_r(r), \tag{33}$$

where the expression of f_r is given Appendix B.

A (regular) fixed points of Eq. (33) is defined as the roots of the following nonlinear equations in presence of constraint

$$f_r(r) = 0 \quad \text{with} \quad \frac{dH(r)}{dr} \neq 0. \tag{34}$$

Assuming $\epsilon \ll 1$, a fixed point of Eq. (33) is an ϵ-approximation of a fixed point of Eq. (19) which characterizes a periodic solution of Eq. (14). As usual, stability of the fixed points are found looking for the sign of $\frac{d}{dr}\left(\frac{f_r(r)}{H'(r)}\right)$.

A singular fixed points of Eq. (33) is defined as the roots of the following nonlinear equations

$$f_r(r) = 0 \quad \text{and} \quad \frac{dH(r)}{dr} = 0. \tag{35}$$

Assuming condition (30), singular fixed points can exists among the fold points defined Eq. (29).

3.4 Prediction of the mitigation limit

Four main types of response regimes may be observed when a NES is attached on an unstable system: complete suppression of the instability, mitigation through Periodic Response (PR), mitigation through Strongly

Modulated Response (SMR) or no mitigation. These four types of responses have been observed and analyzed in the case of a Van de Pol oscillator coupled to one NES [15]. They have been also observed by Bergeot et al. [1] studying mitigation of a mode-coupling instability in breaking systems using two NESs. In the present study we classify these regimes into two categories depending on the fact that the NES acts or not and therefore separating harmless situations from harmful situations:

1. **Harmless situation:** the NES acts resulting to the following regimes
   (a) *Complete suppression.* The trivial fixed point of the slow-flow is reached. In this case, due to the additional damping, the NES attachment stabilizes the system, i.e. the trivial fixed point, common to both the non-averaged system and the slow-flow, becomes stable.
   (b) *Mitigation through Periodic Response.* A nontrivial stable fixed point of the slow-flow is reached. In this case, the steady-state of the non-averaged system response regime is a periodic regime, i.e. LCOs with an amplitude smaller than amplitude of the LCOs undergone by the primary system.
   (c) *Mitigation through Strongly Modulated Response.* In this case, the steady-state response regime is a quasiperiodic regime which exhibits a "fast" component and a "slow" component corresponding to the envelope of the signal. The term "Strongly modulated response" has been introduced in [16] for the study of a harmonically forced linear system coupled to a NES. SMR for the non-averaged system corresponds to relaxation oscillation of the slow-flow. To ensure the existence of SMRs, condition (30) must be respected.
2. **Harmful situation:** the NES does not act resulting to
   (a) *No mitigation.* The NES is not able to mitigate the instability and the non-averaged system saturates on a LCO which has an amplitude close to that of the case without NES. Regarding the slow-flow, it reaches a stable fixed point with large amplitude.

The nature of the steady-state regime depends on two things about the slow-flow. Firstly, it depends on the initial conditions to know where the slow dynamics leads the trajectory on S. Secondly, it depends on the fixed points (position and stability) which orientates the dynamics on S at the slow time scale. Here, for convenience and in accordance with real word situations, we consider a set of initial conditions $\{s(0), r(0)\}^t$ as a small perturbation of the trivial solution $\mathbf{0}$.

Considering the two situations described above and the previous comments, the **mitigation limit** with respect to the friction parameter γ (the chosen bifurcation parameter in this work) is introduced in the following definition. The definition can be adapted to other parameters.

Definition 3.1 *Considering a set of initial conditions (for the slow-flow) $\{s(0), r(0)\}^t$ as a small perturbation of the trivial solution $\mathbf{0}$, the **mitigation limit** of the friction parameter γ is defined as the value of γ , denoted γ_{ml}, which separates harmful situations from harmless situations.*

The definition 3.1 is based only on the nature of the steady-state regimes when 1:1 resonance occurs. This may be questioned regarding the amplitudes of these regimes but it is admitted in this study.

The method to predict the steady-state regimes, and consequently the mitigation limit, is now presented. As a result of the reduction method presented in Sect. 2.2, the slow-flow (17) is equivalent to that of a 1 DOF primary system coupled to one NES. This allows to predict easily the nature of the steady-state regimes. In keeping with [15], conditions to ensure that the system undergoes a harmless situation are stated below assuming that the NES respects condition (30).

Result 3.1 *The conditions to obtain **harmless situations** are split in two cases:*

Case a. *We assume that the slow-flow has a stable fixed point $\{s_s^*, r_s^*\}$ (trivial or nontrivial) on the first attractive part of the critical manifold S. In this case, the system is in a* ***harmless situation*** *if*

$$r_s^* < r^M. \tag{36}$$

In this case harmless situation corresponds to Complete suppression for the trivial fixed point or Mitigation through Periodic Response for the nontrivial fixed points.
If (36) *is not respected one must pass to Case b.*

Case b. *We assume that the system has at least one nontrivial unstable fixed points on a stable part of the critical manifold S; denoted $\{s_u^*, r_u^*\}$. In this case, the system is in an* ***harmless situation*** *if*

$$r_u^* < r^u. \tag{37}$$

In this case harmless situation corresponds to Mitigation through Periodic Response or Mitigation through Strongly Modulated Response.

Conversely, the system is in an ***harmful situation*** *if the system is nether in Case a, nor in Case b.*

We give now a quantitative definition of the *mitigation limit* γ_{ml} of the system.

Result 3.2 *Let γ_{lim}, the value of the parameter γ after which the slow-flow has no more nontrivial unstable fixed points and γ^s the value of the parameter γ such that*

$$r_u^* = r^u, \tag{38}$$

where r^u is defined by Eq. (31)*.*

The theoretical prediction of the mitigation limit, denoted γ_{ml}^{th}, is defined as follows

$$\gamma_{ml}^{th} = \begin{cases} \gamma^s, & \text{if } \gamma^s < \gamma_{lim} \quad (39a) \\ \gamma_{lim}, & \text{if } \gamma^s > \gamma_{lim}. \quad (39b) \end{cases}$$

4 Numerical illustrations of the steady-state response regimes

The purpose of this section is to illustrate some steady-state response regimes by means of direct numerical integration of the FNAS (10), the RNAS (14) and the slow-flow (17). To achieve this, the following set of parameters is used

$$\eta_1 = 0.4,\ \eta_1 = 1,\ \varphi_1 = 8,\ \varphi_2 = 2,\ \epsilon = 0.01,\ \alpha = 4 \tag{40}$$

with $\mu = 0.35$ and for three de different values of γ: 1.5, 1.67 and 2 leading respectively to *Mitigation through Periodic Response*, Mitigation through Strongly Modulated Response and *No mitigation* of the LCO (see Fig 3). As expected the RNAS is a good approximation of the FNAS during transient and it is valid during steady-state regime only when the latter has a relatively small amplitude, as it is here for *Mitigation through Periodic Response*. On the other hand, the slow-flow appears to be alway a good approximation of the RNAS.

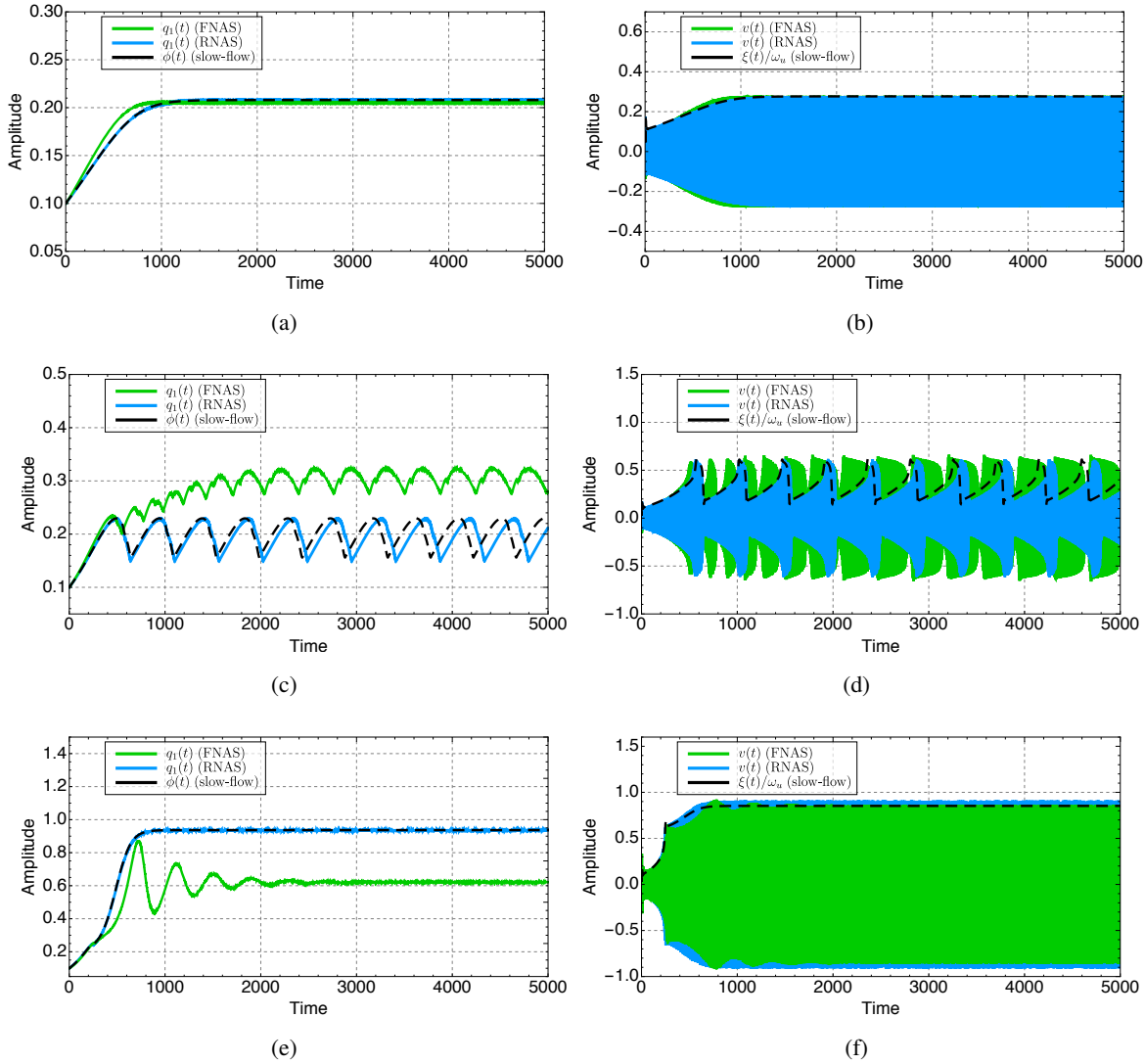

Figure 3: Direct numerical integration of the FNAS (10), the RNAS (14) and of the slow-flow (17). Set of parameters (40) is used with $\mu = 0.35$. (a) and (b) $\gamma = 1.5$; (c) and (d) $\gamma = 1.67$; (e) and (f) $\gamma = 2$.

5 Comparison of theoretical results with numerical simulations

In this section, analytical predictions proposed in Results 3.1 and 3.2 are compared to direct numerical integration of the system.

The comparison between the theoretical bifurcation diagram, obtained from Eq. (34) and the maximum steady-state amplitudes obtained from numerical simulations of the Full Non-Averaged System (FNAS) (10), the Reduced Non-Averaged System (RNAS) (14) and of the slow-flow (17b) using the set of parameters (40) is presented in Figs. 4 and 5 for different values of the NES parameter μ. The graphs of the maximum steady-state amplitude give a numerical estimation of the mitigation limit as the value of γ for which the last jump of the amplitude is observed.

In Fig 4, where $\mu = 0.35$, the amplitude jump appears at $\gamma \approx 1.67$ for the FNAS and at $\gamma \approx 1.74$ for both the RNAS and the slow-flow (see the last jump of the amplitude of the variable s Fig 4(a) and r Fig 4(b). Hence the reduction of the dynamic causes here a slight increase in the value of the mitigation limit. However, the slow-flow, can predict the mitigation limit observed with the RNAS. Previous values must be compared to the theoretical prediction $\gamma_{ml}^{th} \approx 1.72$ which is given, for $\mu = 0.35$, by Eq. (39a). Here γ_s is obtained solving Eq. (38) graphically in Fig. 4(b) as the intersection of the branch of the larger unstable fixed points (dark

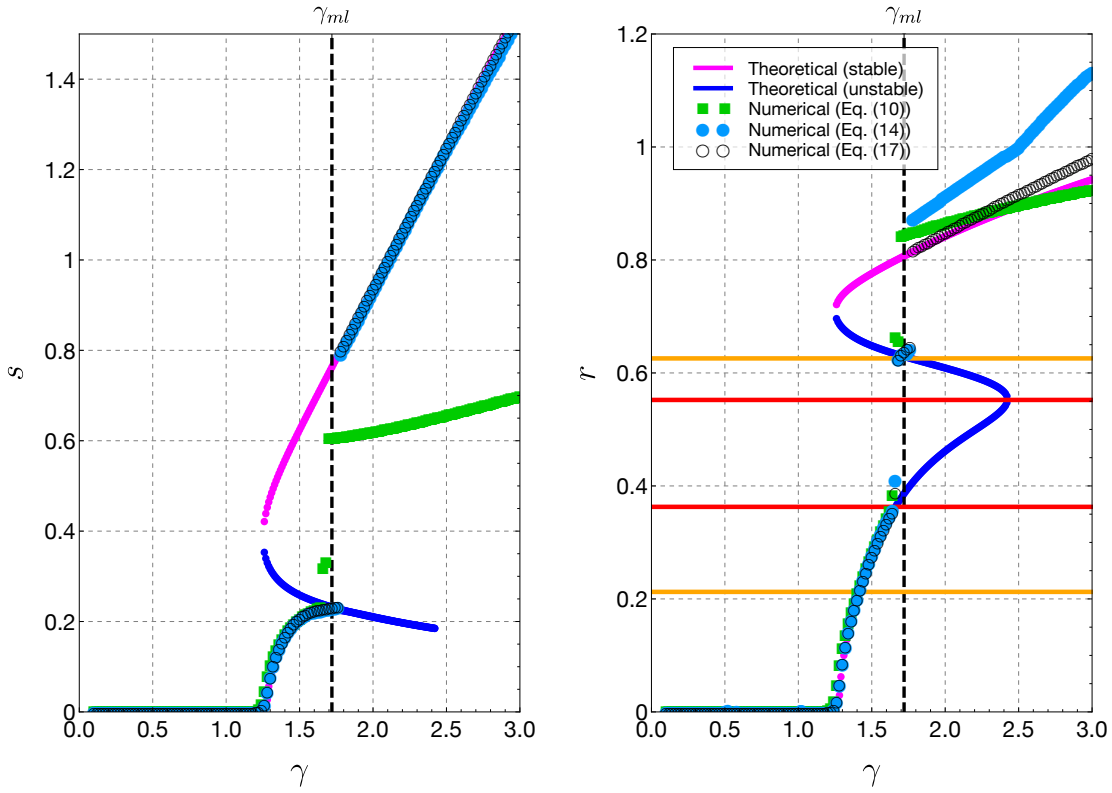

(a) (b)

Figure 4: Comparison between theoretical bifurcation diagram (magenta dots for stable fixed points and blue dots for unstable fixed points) and maximum steady-state amplitudes obtained from numerical simulations of the Eq. (10) (green filled squares), Eq. (14) (blue filled circles) and Eq. (17) (black empty circles). Bifurcation diagram and maximum steady-state amplitudes are plotted for the variables (a) s and (b) r. In the latter, red horizontal lines correspond to r^M and r^m (with $r^M < r^m$) and orange horizontal lines correspond to r^u and r^d (with $r^d < r^u$). Set of parameters (40) is used with $\mu = 0.35$.

blue curve) and r^u (upper orange horizontal line). Therefore, a good agreement between prediction and direct numerical simulations is observed. Moreover, we can state here the same conclusion about amplitudes as in Sect. 4, with, in addition, a significant difference observed between the amplitude of the slow-flow and that of the RNAS after the jump. This can be due to the fact that the assumption of 1:1 resonance capture is not respected anymore. Indeed, an FFT performed on the signals shows the appearance of additional harmonics in the steady-state response regimes of the RNAS. Note that these harmonics are not present in the steady-state response regimes of the FNAS. However, all these differences do not affect the good prediction of the mitigation limit.

In Fig 5, only graphs with respect to the variable r are presented with $\mu \approx 0.4$, 0.45 and 0.57. One can see that the last amplitude jump appears at $\gamma \approx 1.85$, 1.94 and 1.9 for both the RNAS and the slow-flow and they are well predicted by the theoretical values ($\gamma_{ml}^{th} \approx 1.87$, 1.98 and 1.95 respectively[2]). These results allows to validate the asymptotic study presented in Sect. 3.

However, the comparison between the mitigation limits observed on the graph of the maximum steady-state amplitudes of the FNAS (the amplitude jump appears at $\gamma = 1.67$, 1.65 and 1.63) and the theoretical prediction highlights the limits of the dynamics reduction method presented in Sect. 2.2. Indeed, the theoretical values overestimate now the mitigation limit observed with FNAS when μ increases. The overestimation of

[2]When $\mu = 0.4$ and 0.45, the theoretical prediction γ_{ml}^{th} is given by Eq. (39a) whereas it is given by Eq. (39b) for $\mu = 0.57$. Like γ_s, the value of γ_{lim} is determined graphically.

the mitigation is due to a bad estimation of amplitudes before the jump (see Fig. 5), even if the amplitudes are small. The causes of these discrepancies are not yet known, this will be subject of future work.

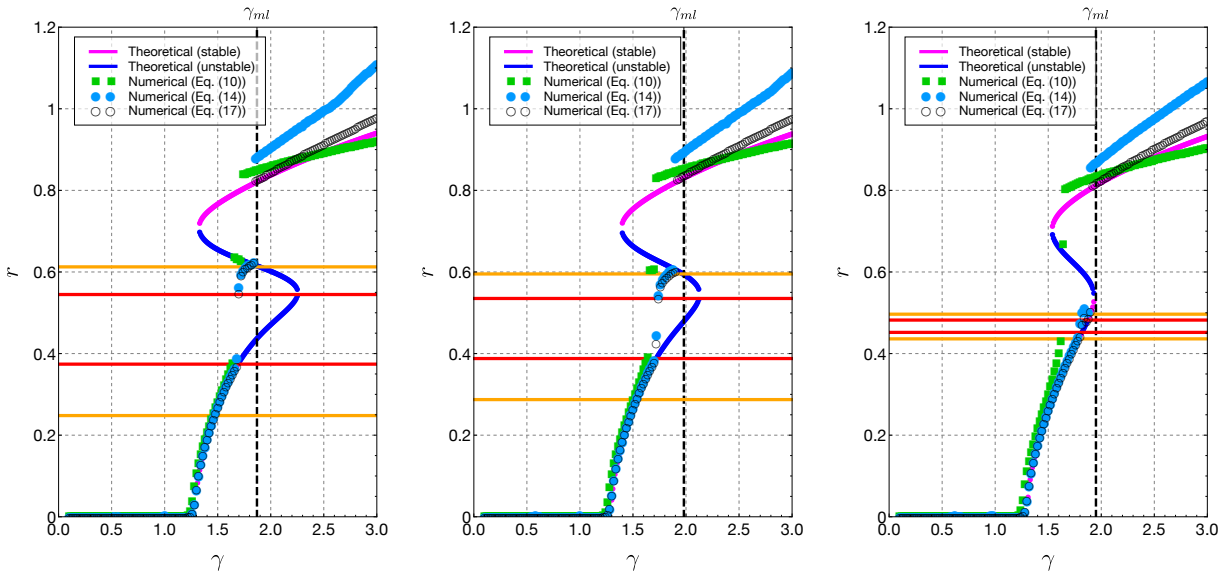

Figure 5: Same caption as for Fig. 4(b) with $\mu = 0.4$, 0.45 and 0.57.

6 Conclusion

We studied the capacity of Nonlinear Energy Sinks (NES) to mitigate vibrations due to mode-coupling instability in braking systems. As an extension of a previous work [1], we used here a general dynamics reduction method allowing to obtain a one dimensional critical manifolds and consequently to predict all the steady-state response regimes observed using direct numerical integration of the equations of motion. In particular, the mitigation limit, defined as the value of the friction coefficient which separates harmful situations from harmless situations, has been predicted. The comparison with numerical simulation allows to validate the used asymptotic analysis but highlights the limits of the dynamic reduction method. Indeed, overestimations of the mitigation limit are observed for large value of NES damping parameter. The causes of these discrepancies are not yet known and will be subject of future work.

A Slow-fast system

The function f, g_1 and g_2 characterizing the slow-fow system (19) are given here after.

$$
\begin{aligned}
f(s,r,\delta) \;=\; & \frac{1}{2}\Big(2s\rho_u - r\cos(\delta)\mathbf{l}_{31}^I + r\sin(\delta)\mathbf{l}_{31}^R - 2s\mathbf{l}_{31}^I\mathbf{r}_{11}^I + 2s\mathbf{l}_{31}^R\mathbf{r}_{11}^R \\
& -6s^3\mathbf{l}_{31}^I\mathbf{r}_{11}^{I^2}\mathbf{r}_{12}^I\varphi_1 + 12s^3\mathbf{r}_{11}^I\mathbf{r}_{12}^I\mathbf{l}_{31}^R\mathbf{r}_{11}^R\varphi_1 + 6s^3\mathbf{l}_{31}^I\mathbf{r}_{12}^I\mathbf{r}_{11}^{R^2}\varphi_1 \\
& +6s^3\mathbf{r}_{11}^{I^2}\mathbf{l}_{31}^R\mathbf{r}_{12}^R\varphi_1 + 12s^3\mathbf{l}_{31}^I\mathbf{r}_{11}^I\mathbf{r}_{11}^{R^2}\mathbf{r}_{12}^R\varphi_1 - 6s^3\mathbf{l}_{31}^R\mathbf{r}_{11}^R\mathbf{r}_{12}^R\varphi_1 \\
& -6s^3\mathbf{l}_{41}^I\mathbf{r}_{21}^{I^2}\mathbf{r}_{22}^I\varphi_2 + 12s^3\mathbf{r}_{21}^I\mathbf{r}_{22}^I\mathbf{l}_{41}^R\mathbf{r}_{21}^R\varphi_2\omega_u + 6s^3\mathbf{l}_{41}^I\mathbf{r}_{22}^I\mathbf{r}_{21}^{R^2}\varphi_2\omega_u \\
& +6s^3\mathbf{r}_{21}^{I^2}\mathbf{l}_{41}^R\mathbf{r}_{22}^R\varphi_2\omega_u + 12s^3\mathbf{l}_{41}^I\mathbf{r}_{21}^I\mathbf{r}_{21}^R\mathbf{r}_{22}^R\varphi_2\omega_u \\
& -6s^3\mathbf{l}_{41}^R\mathbf{r}_{21}^{R^2}\mathbf{r}_{22}^R\varphi_2\omega_u\Big)
\end{aligned}
\tag{41}
$$

$$
\begin{aligned}
g_1(s,r,\delta,\epsilon) \quad &= -\frac{r\mu}{2} + s\sin(\delta)\mathbf{r}_{11}^{I} - s\cos(\delta)\mathbf{r}_{11}^{R} + \epsilon\left(-\frac{r\mu}{2} - s\sin(\delta)\mathbf{r}_{11}^{I} - s\gamma\sin(\delta)\mathbf{r}_{21}^{I}\right.\\
&+s\eta_1\sin(\delta)\mathbf{r}_{31}^{I} - s\eta_1\cos(\delta)\mathbf{r}_{31}^{R} + s\cos(\delta)\mathbf{r}_{11}^{R} + s\gamma\cos(\delta)\mathbf{r}_{21}^{R}\\
&-3s^3\sin(\delta)\mathbf{r}_{11}^{I^2}\mathbf{r}_{12}^{I}\varphi_1 + 6s^3\cos(\delta)\mathbf{r}_{11}^{I}\mathbf{r}_{12}^{I}\mathbf{r}_{11}^{R}\varphi_1 + 3s^3\sin(\delta)\mathbf{r}_{12}^{I}\mathbf{r}_{11}^{R^2}\varphi_1\\
&\left.+3s^3\cos(\delta)\mathbf{r}_{11}^{I^2}\mathbf{r}_{12}^{R}\varphi_1 + 6s^3\sin(\delta)\mathbf{r}_{11}^{I}\mathbf{r}_{11}^{R}\mathbf{r}_{12}^{R}\varphi_1 - 3s^3\cos(\delta)\mathbf{r}_{11}^{R^2}\mathbf{r}_{12}^{R}\varphi_1\right) \qquad (42)
\end{aligned}
$$

$$
\begin{aligned}
g_2(s,r,\delta,\epsilon) \quad &= \quad \frac{-3r^3\alpha + 8s\cos(\delta)\mathbf{r}_{11}^{I} + 8s\sin(\delta)\mathbf{r}_{11}^{R} + 4r}{8r}\\
&+\epsilon\left(\frac{1}{2s}\left(2s\nu_u + r\sin(\delta)\mathbf{l}_{31}^{I} + r\cos(\delta)\mathbf{l}_{31}^{R} + 2s\mathbf{r}_{11}^{I}\mathbf{l}_{31}^{R} + 2s\mathbf{l}_{31}^{I}\mathbf{r}_{11}^{R}\right.\right.\\
&+6s^3\mathbf{r}_{11}^{I^2}\mathbf{r}_{12}^{I}\mathbf{l}_{31}^{R}\varphi_1 + 12s^3\mathbf{l}_{31}^{I}\mathbf{r}_{11}^{I}\mathbf{r}_{12}^{I}\mathbf{r}_{11}^{R}\varphi_1 - 6s^3\mathbf{r}_{12}^{I}\mathbf{l}_{31}^{R}\mathbf{r}_{11}^{R^2}\varphi_1\\
&+6s^3\mathbf{l}_{31}^{I}\mathbf{r}_{11}^{I^2}\mathbf{r}_{12}^{R}\varphi_1 - 12s^3\mathbf{r}_{11}^{I}\mathbf{l}_{31}^{R}\mathbf{r}_{11}^{R}\mathbf{r}_{12}^{R}\varphi_1 - 6s^3\mathbf{l}_{31}^{I}\mathbf{r}_{11}^{R^2}\mathbf{r}_{12}^{R}\varphi_1\\
&+6s^3\mathbf{r}_{21}^{I^2}\mathbf{r}_{22}^{I}\mathbf{l}_{41}^{R}\varphi_2 + 12s^3\mathbf{l}_{41}^{I}\mathbf{r}_{21}^{I}\mathbf{r}_{22}^{I}\mathbf{r}_{21}^{R}\varphi_2 - 6s^3\mathbf{r}_{22}^{I}\mathbf{l}_{41}^{R}\mathbf{r}_{21}^{R^2}\varphi_2\\
&\left.+6s^3\mathbf{l}_{41}^{I}\mathbf{r}_{21}^{I^2}\mathbf{r}_{22}^{R}\varphi_2 - 12s^3\mathbf{r}_{21}^{I}\mathbf{l}_{41}^{R}\mathbf{r}_{21}^{R}\mathbf{r}_{22}^{R}\varphi_2 - 6s^3\mathbf{l}_{41}^{I}\mathbf{r}_{21}^{R^2}\mathbf{r}_{22}^{R}\varphi_2\right)\\
&+\frac{1}{8r}\left(-3r^3\alpha - 4r - 8s\cos(\delta)\mathbf{r}_{11}^{I} - 8s\gamma\cos(\delta)\mathbf{r}_{21}^{I} + 8s\eta_1\cos(\delta)\mathbf{r}_{31}^{I}\right.\\
&-8s\sin(\delta)\mathbf{r}_{11}^{R} - 8s\gamma\sin(\delta)\mathbf{r}_{21}^{R} + 8s\eta_1\sin(\delta)\mathbf{r}_{31}^{R} - 24s^3\cos(\delta)\mathbf{r}_{11}^{I^2}\mathbf{r}_{12}^{I}\varphi_1\\
&-48s^3\sin(\delta)\mathbf{r}_{11}^{I}\mathbf{r}_{12}^{I}\mathbf{r}_{11}^{R}\varphi_1 + 24s^3\cos(\delta)\mathbf{r}_{12}^{I}\mathbf{r}_{11}^{R^2}\varphi_1 - 24s^3\sin(\delta)\mathbf{r}_{11}^{I^2}\mathbf{r}_{12}^{R}\varphi_1\\
&\left.\left.+48s^3\cos(\delta)\mathbf{r}_{11}^{I}\mathbf{r}_{11}^{R}\mathbf{r}_{12}^{R}\varphi_1 + 24s^3\sin(\delta)\mathbf{r}_{11}^{R^2}\mathbf{r}_{12}^{R}\varphi_1\right)\right) \qquad (43)
\end{aligned}
$$

B Slow subsystem

The function f_r characterizing Eq. (33) is given here after.

$$
\begin{aligned}
f_r(r) \quad &= \quad \frac{r^2}{8\left(\mathbf{r}_{11}^{I^2} + \mathbf{r}_{11}^{R^2}\right)}\left\{-4\left(\mu^2 + 4\left(\frac{3r^2\alpha}{8} - \frac{1}{2}\right)^2\right)\right.\\
&\left[\left(\mathbf{r}_{11}^{I^2} + \mathbf{r}_{11}^{R^2}\right)\left(-\rho_u + \mathbf{l}_{31}^{R}\left(-\mathbf{r}_{11}^{R} - \frac{3}{4}r^2\mathbf{r}_{12}^{R}\varphi_1\left(\mu^2 + 4\left(\frac{3r^2\alpha}{8} - \frac{1}{2}\right)^2\right)\right)\right)\right.\\
&+\mathbf{l}_{31}^{I}\left(\mathbf{r}_{11}^{I}\left(\mathbf{r}_{11}^{I^2} + \mathbf{r}_{11}^{R^2}\right) + \frac{3}{4}r^2\left(\mathbf{r}_{12}^{I}\left(\mathbf{r}_{11}^{I^2} - \mathbf{r}_{11}^{R^2}\right) - 2\mathbf{r}_{11}^{I}\mathbf{r}_{11}^{R}\mathbf{r}_{12}^{R}\right)\varphi_1\left(\mu^2 + 4\left(\frac{3r^2\alpha}{8} - \frac{1}{2}\right)^2\right)\right)\\
&-\frac{3}{2}r^2\mathbf{r}_{11}^{I}\mathbf{r}_{12}^{I}\mathbf{l}_{31}^{R}\mathbf{r}_{11}^{R}\varphi_1\left(\mu^2 + 4\left(\frac{3r^2\alpha}{8} - \frac{1}{2}\right)^2\right) + \frac{3}{4}r^2\left(\mathbf{l}_{41}^{I}\left(\mathbf{r}_{22}^{I}\left(\mathbf{r}_{21}^{I^2} - \mathbf{r}_{21}^{R^2}\right) - 2\mathbf{r}_{21}^{I}\mathbf{r}_{21}^{R}\mathbf{r}_{22}^{R}\right)\right.\\
&\left.\left.+\mathbf{l}_{41}^{R}\left(-2\mathbf{r}_{21}^{I}\mathbf{r}_{22}^{I}\mathbf{r}_{21}^{R} + \left(-\mathbf{r}_{21}^{I^2} + \mathbf{r}_{21}^{R^2}\right)\mathbf{r}_{22}^{R}\right)\right)\varphi_2\left(\mu^2 + 4\left(\frac{3r^2\alpha}{8} - \frac{1}{2}\right)^2\right)\right]\\
&-\left(\mathbf{r}_{11}^{I^2} + \mathbf{r}_{11}^{R^2}\right)\\
&\left.\left[\mathbf{l}_{31}^{I}\left(-4\mu\mathbf{r}_{11}^{R} + \mathbf{r}_{11}^{I}\left(3r^2\alpha - 4\right)\right) + \mathbf{l}_{31}^{R}\left(-4\mu\mathbf{r}_{11}^{I} + \mathbf{r}_{11}^{R}\left(-3r^2\alpha + 4^4\right)\right)\right]\right\} \qquad (44)
\end{aligned}
$$

References

[1] B Bergeot, S Berger, and S Bellizzi. Mode coupling instability mitigation in friction systems by means of nonlinear energy sinks : numerical highlighting and local stability analysis. *Journal of Vibration and Control*, 2017.

[2] L. Nechak, S. Berger, and E. Aubry. Non-intrusive generalized polynomial chaos for the robust stability analysis of uncertain nonlinear dynamic friction systems. *Journal of Sound and Vibration*, 332(5):1204–1215, 2013.

[3] L. Nechak and J. J. Sinou. Hybrid surrogate model for the prediction of uncertain friction-induced instabilities. *Journal of Sound and Vibration*, 396:122–143, 2017.

[4] Oberst S and J.C.S Lai. Statistical analysis of brake squeal noise. *Journal of Sound and Vibration*, 330:2978–2994, 2011.

[5] A.F. D'Souza and A.H. Dweib. Self-excited vibrations induced by dry friction, part 2: Stability and limit-cycle analysis. *Journal of Sound and Vibration*, 137(2):177–190, 1990.

[6] M Eriksson and S Jacobson. Friction behaviour and squeal generation of disc brakes at low speeds. *Proceedings of the Institution of Mechanical Engineers, Part D: Journal of Automobile Engineering*, 215(12):1245–1256, 2001.

[7] N Hoffmann and L Gaul. Effects of damping on mode-coupling instability in friction induced oscillations. *{ZAMM} - Journal of Applied Mathematics and Mechanics / Zeitschrift für Angewandte Mathematik und Mechanik*, 83(8):524–534, 2003.

[8] N.M. Kinkaid, O.M. O'Reilly, and P. Papadopoulos. Automotive disc brake squeal. *Journal of Sound and Vibration*, 267:105–166, 2003.

[9] A.F. Vakakis and O.V. Gendelman. Energy pumping in nonlinear mechanical oscillators: Part II - Resonance capture. *Journal of Applied Mechanics*, 68:42–48, 2001.

[10] A. F. Vakakis, O. V. Gendelman, L. A. Bergman, D. M. McFarland, G. Kerschen, and Y. S. Lee. *Nonlinear Targeted Energy Transfer in Mechanical and Structural Systems*. Springer-Verlag, Berlin, New York, 2008.

[11] J. Hultén. Friction phenomena related to drum brake squeal instabilities. In *ASME Design Engineering Technical Conferences, Sacramento, CA*, 1997.

[12] L. Meirovitch. *Fundamentals of Vibrations*, chapter 7. McGraw-Hill, 2001.

[13] N Fenichel. Geometric singular perturbation theory for ordinary differential equations. *Journal of Differential Equations*, 98:53–98, 1979.

[14] C.K.R.T. Jones. Geometric singular perturbation theory. In Russell Johnson, editor, *Dynamical Systems*, volume 1609 of *Lecture Notes in Mathematics*, pages 44–118. Springer Berlin Heidelberg, 1995.

[15] O. V. Gendelman and T. Bar. Bifurcations of self-excitation regimes in a Van der Pol oscillator with a nonlinear energy sink. *Physica D*, 239(3-4):220–229, February 2010.

[16] Y. Starosvetsky and O. V. Gendelman. Strongly modulated response in forced 2dof oscillatory system with essential mass and potential asymmetry. *Physica D*, 237(13):1719–1733, August 2008.